PROCEEDINGS OF SPIE

SST and cloud mask algorithms in reprocessing 1981-2002 NOAA AVHRR data for SST with the Advanced Clear-Sky Processor for Oceans (ACSPO)

Petrenko, B., Pryamitsyn, V., Ignatov, A., Kihai, Y.

SPIE.

SST and Cloud Mask Algorithms in Reprocessing 1981-2002 NOAA AVHRR Data for SST with the Advanced Clear-Sky Processor for Oceans (ACSPO)

B. Petrenko[1,2], V. Pryamitsyn[1,2], A. Ignatov[1] and Y. Kihai[1,2]

[1]NOAA STAR, [2]GST, Inc.

ABSTRACT

The goal of the NOAA AVHRR GAC Reanalysis (RAN) project is to create long-term time series of uniform sea surface temperature (SST) retrievals (Level 2 and 3 products) from AVHRR data using the Advanced Clear-Sky Processor for Oceans (ACSPO) system. During Phase 1 ('RAN1'), data of several AVHRR/3s from 2002-2015 were reprocessed. Ongoing Phase 2 ('RAN2') aims to cover the full period of AVHRR GAC data from 1981-on. At the time of this writing, we reprocessed five AVHRR/2s onboard NOAA-07, -09, -11, -12 and -14 and two AVHRR/3s onboard NOAA-15 and -16, and created an initial "beta" RAN2 data set ('RAN2 B01') spanning ~22 years from 1981-2003. The ACSPO algorithms for cloud masking and training SST regression coefficients, initially developed for operational SST processing, required modifications to mitigate the issues, specific to the RAN2 period: multiple sensor issues, and insufficient number of *in situ* SST data and their degraded quality. Another derived complexity, also related to insufficient and poor quality of satellite and *in situ* data, is the limited availability and suboptimal quality of first guess SSTs, which is used in ACSPO for cloud masking and quality control, and employed in the right part of the Non-Linear SST equations. The paper describes modifications to the ACSPO algorithms made for the RAN2 B01, and demonstrates the resulting improvements in the retrieved SST.

1. INTRODUCTION

Starting with the NOAA-07, launched in September 1981, multiple NOAA satellites, as well as European satellites Metop-1, -2 and -3, carried the Advanced Very High Resolution Radiometers, AVHRR/2 and /3, suitable for SST retrievals from spectral bands 3/3b, 4 and 5, centered at 3.7, 10.8 and 12 μm, respectively. The NOAA AVHRR GAC SST Reanalysis (RAN) project [1], along with two other AVHRR reprocessing efforts [2-3], is aimed at creating a uniform ~40 year-long global SST dataset in support of long-term/climate studies and applications from NOAA AVHRR data in the 4 km Global Area Coverage (GAC) mode since 1981-on. Earlier, under Reanalysis Version 1 (RAN1), the data of AVHRR/3s onboard NOAA-16, 17, 18 and 19, and Metop-A satellites from 2002-2015 were reprocessed with the Advanced Clear-Sky Processor for Oceans (ACSPO) system [1]. The goal of the ongoing Reanalysis Version 2 (RAN2) is to cover the full period of AVHRR GAC SST data from NOAA AVHRR/2s and AVHRR/3s. The Metop AVHRR/3s data in 1 km Full-Resolution Area Coverage (FRAC) mode, are not included in this GAC RAN2, and will be reprocessed separately as a part of FRAC RAN1. As of this writing, an initial version of the AVHRR GAC RAN2 SST data set ('RAN2 B01') was created, covering a period from 1981-2003. The core ACSPO SST retrieval, training and cloud masking algorithms [5-8], originally developed for near-real time (NRT) SST retrievals from newer satellites, were modified to mitigate the following issues intrinsic to the earlier AVHRRs and to the auxiliary data during this period:

- The effect of AVHRR sensors instabilities on retrieved SST is minimized, by recalculation of regression coefficients on a daily basis using matchup data sets (MDSs) of clear-sky AVHRR brightness temperatures (BTs) with *in situ* SSTs, collected within a sliding time window centered at the processed day. This approach was earlier used in RAN1 for one out of two ACSPO SST products - Global Regression (GR) SST. In RAN2, it was implemented for both ACSPO SST products, GR SST and Piecewise Regression (PWR) SSTs.

- The occasional outliers in the band 3b on the earlier AVHRRs', caused by Sun impingement on the sensor, are screened out with sensor-specific "Warm Outliers" filter incorporated in the ACSPO Clear-Sky Mask (ACSM).

- The sensitivity of retrieved "sub-skin" SST to true SST is maintained at a pre-defined level, by calculating regression coefficients under a constraint on mean sensitivity over a training MDS. Note that constraining the sensitivity to true SST also limits its sensitivity to the "first-guess" SST, used in the non-linear NLSST equations. This is especially important for the RAN2 B01 period because of suboptimal quality of available L4 SST analyses.

- The ACSPO regression SST algorithms are customarily trained against *in situ* data from drifters and moored buoys (D+TM). Due to the critical shortage of *in situ* data of these types in the 1980-90s, less accurate but more numerous ship (S) SSTs were added to the training MDS (D+TM+S), when processing data of NOAA-07, -09 and -11.

This paper describes the modifications to ACSPO algorithms implemented in RAN2 B01, demonstrates their effects on retrieved SST and outlines problems yet to be solved. The detailed cross-evaluation of the RAN2 B01 SST, including comparisons with the two other available long-term AVHRR SST data sets, NOAA/NASA Pathfinder v. 5.3 (PF) [3] and ESA Climate Change Initiative v.2.1 (CCI) [3], is found in [4].

2. DATA

2.1 AVHRR data

Table 1 lists the NOAA satellites processed in RAN2 B01, types of the AVHRR instruments, types of orbits (morning or afternoon, at the beginning of the mission), periods of L1b data availability, and periods processed in ACSPO. The periods, when the quality of the AVHRR data was unacceptably low, were excluded from the RAN2 B01. For all satellites except NOAA-07, SST was retrieved from three IR bands at night and two longwave bands 4 and 5 during the day. For NOAA-07, the two latter bands were used for SST during both day and night, because of the permanent failure of band 3b in September 1982 (see NOAA 3S system, available at https://www.star.nesdis.noaa.gov/sod/sst/3s/, [9]). The daytime and nighttime algorithms were switched at solar zenith angle, SZA=90°.

Table 1. NOAA satellites employed in RAN2 B01, periods of L1b data availability and periods processed.

| Satellite	Orbit	Sensor	L1b data available	Used in RAN2 B01
NOAA-07	Afternoon	AVHRR/2	01 Sep 1981 – 02 Feb 1985	01 Sep 1981 – 02 Feb 1985
NOAA-09	Afternoon	AVHRR/2	25 Feb 1985 – 07 Nov 1988	25 Feb 1985 – 07 Nov 1988
NOAA-11	Afternoon	AVHRR/2	08 Nov 1988 – 31 Dec 1994	08 Nov 1988 – 13 Sep 1994
NOAA-12	Morning	AVHRR/2	16 Sep 1991 – 14 Dec 1998	16 Sep 1991 – 13 Dec 1998
NOAA-14	Afternoon	AVHRR/2	01 Jan 1995 – 08 Oct 2002	20 Jan 1995 – 31 Oct 2001
NOAA-15	Morning	AVHRR/3	01 Nov 1998 – 31 Dec 2018	01 Nov 1998 – 22 Nov 2000, 24 Jan 2001 – 26 Oct 2003
NOAA-16	Afternoon	AVHRR/3	01 Jan 2001 – 22 Aug 2009	02 Jan 2001 – 31 Dec 2002
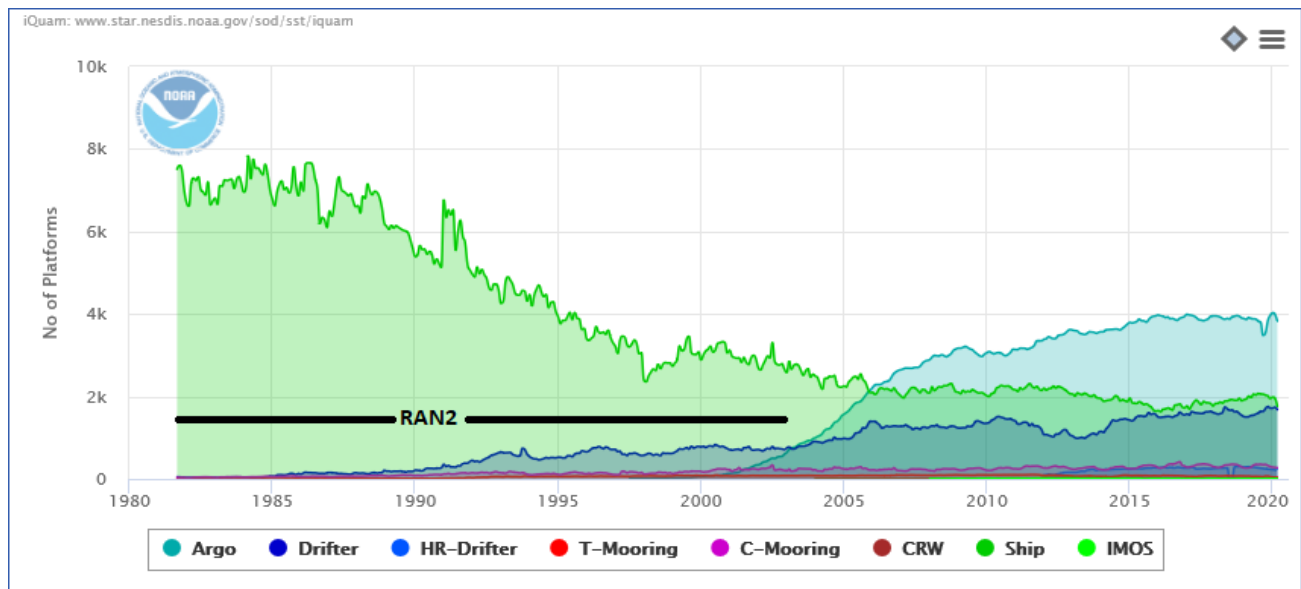
Figure 1. Monthly numbers of in situ platform IDs for 1981-2020 from iQuam, www.star.nesdis.noaa.gov/socd/sst/iquam/ [10].

2.2 *In situ* SSTs

Regression SST coefficients in ACSPO are customarily derived from matchups of clear-sky satellite BTs with drifting and tropical moored buoys (hereafter, "D+TM"). The quality controlled *in situ* data obtained from the NOAA *i*Quam system www.star.nesdis.noaa.gov/sod/sst/iquam/ [10] are used for validation. Results of validation are monitored in another NOAA system, SQUAM, www.star.nsdis.noaa.gov/sod/sst/squam/ [11]. Figure 1 taken from *i*Quam, shows monthly total number of *in situ* platform IDs of different types in 1981-2020. During the RAN2 B01 period 1981-2003, the monthly numbers of D+TM measurements do not exceed several hundred and quickly decrease when moving back in time, especially in the 1980s. Matching these measurements with clear-sky satellite BTs further reduces the numbers of usable *in situ* data by ~80 to 90%, making the D+TM combination insufficient for training (and validation) purposes. On the other hand, in 1981-2003 (especially in 1981-1991) the monthly number of ships (S) far exceeds the number of D+TM. Despite relatively low precision of the ship SST measurements ~1 K (e.g., [12]), adding them to training datasets of matchups (MDS) was found beneficial for NOAA-07, -09 and -11 (D+TM+S). For the newer satellites, NOAA-12, 14, 15 and 16, only D+TM continued to be employed for training as is currently done for the operational products.

2.3 L4 analyses and atmospheric data

The important element of the ACSPO auxiliary data is "first guess" SST, obtained from L4 analyses and employed in the algorithms of the NLSST type [13] and in the ACSPO Clear-Sky Mask (ACSM). The NRT ACSPO employs the Canadian Meteorological Center (CMC) L4 SST [14]. Since the CMC data set starts in September 1991, it was used in RAN2 B01 for satellites launched on or after this date, including NOAA-12, 14, 15 and 16. For the earlier satellites, including NOAA-07, 09 and 11, ESA Climate Change Initiative v.2.1 (CCI) L4 SST was employed, which was available from September 1981 [3]. The CCI data set includes the L2 and L3 "skin" and "depth" SST products, retrieved from NOAA AVHRRs, and the L4 analysis SST produced from these low-level AVHRR products.

In addition to SST retrievals, ACSPO also calculates simulated AVHRR clear-sky brightness temperatures (BTs) using the Community Radiative Transfer Model (CRTM) [15], with "first-guess" L4 analysis and atmospheric profiles of temperature and humidity. Instead of the NCEP Global Forecast System (GFS) profiles employed in operational processing (and also used in AVHRR GAC RAN1, which only extended back to 2002), RAN2 B01 employed profiles from the Modern-Era Retrospective analysis for Research and Applications (MERRA), available back to 1981 at https://gmao.gsfc.nasa.gov/reanalysis/MERRA/ [16]. Model-minus-observation BT biases are monitored in the NOAA Monitoring IR Clear-sky radiances over Ocean for SST (MICROS; www.star.nsdis.noaa.gov/sod/sst/micros/) [17], and were found very helpful to diagnose and empirically mitigate any AVHRR instabilities resulting in BT artifacts [1].

3. SST ALGORITHMS AND TRAINING REGRESSION COEFFICIENTS

ACSPO generates two SST products, with two different algorithms: Global Regression (GR) and Piece-Wise Regression (PWR). Both are trained against *in situ* data, the GR in a global domain and the PWR separately in its various sub-domains.

Although the ACSPO GR SST is referred to as "sub-skin" SST (as it is produced unbiased with respect to *in situ* "depth" SST, T_{DEPTH}, within the global MDS domain), it is more sensitive to spatial variations in "skin" SST, T_{SKIN} [6]. The ACSPO GR designation as "sub-skin" is in contrast with the "skin" SST, T_{SKIN}, produced by the PF and CCI systems, which either calculate the regression SST against *in situ* SST and then de-bias it by subtracting 0.17 K (as it is done in PF), or employ physical retrievals which should result in "skin" SST (CCI).

The second ACSPO product, Piecewise Regression (PWR) SST, is less sensitive to T_{SKIN} but more precise with respect to *in situ* SST, T_{IS} [7]. Because of superior accuracy and precision of fitting *in situ SST*, the ACSPO PWR SST serves as a proxy for T_{DEPTH}.

Both AVHRR products are produced by two- and three-band regression equations.

The two-band SST equation (used for all satellites during day and for NOAA-07 at night) takes the following form:

$$T_S = a_0 + a_1 T_{11} + a_2 (T_{11} - T_{12}) + a_3 T_{11} S + a_4 (T_{11} - T_{12}) S + a_5 (T_{11} - T_{12}) T0 + a_6 S. \tag{1}$$

The three-band equation (used at night for all satellites except NOAA-07) formulates as follows:

$T_S = b_0 + b_1 T_{11} + b_2(T_{11}-T_{3.7}) + b_3(T_{11}-T_{12}) + b_4 T_{11}S + b_5(T_{11}-T_{3.7})S + b_6(T_{11}-T_{12})S + b_7(T_{11}-T_{3.7})T_0 + b_8(T_{11}-T_{12})T_0 + b_9 S.$ (2)

Here, $T_{3.7}$, T_{11} and T_{12} are AVHRR BTs at 3.7, 10.8 and 12 μm; $S = \sec(\theta)-1$, θ is satellite view zenith angle (VZA); a_1, a_2, ..., a_6 and b_1, b_2, ..., b_9 are regression coefficients; a_0 and b_0 are offsets. T_0 is the "first-guess" SST, obtained by interpolation of gridded analysis L4 SST to AVHRR pixels.

The GR SST uses globally two sets of coefficients, one for day and another one for night. Both sets are trained against corresponding global MDSs. The PWR SST uses multiple sets of coefficients, trained against subsets of matchups, whose vectors of regressors, **R,** belong to specific segments in the space of regressors (**R**-space). During retrieval, the coefficients are selected by value of **R** at a given pixel. In NRT ACSPO [7], as well as in AVHRR GAC RAN1 [1], the **R**-space was constructed from all regressors included in a given equation. In RAN2, in order to reduce the dependency of PWR SST on the analysis, the **R**-space was spanned only by those regressors, which are independent of T_0.

Processing data of each satellite takes several runs. On the first run, the full mission is processed with predefined set of "initial" regression coefficients. The resulting "initial" L2P SST retrievals are used to adjust the ACSM filters and to collect matchups of clear-sky AVHRR BTs with *in situ* SST, T_{IS}, from which a new set of regression coefficients is derived. The next pass through the data is performed with these improved coefficients, and the new MDSs are used to derive variable (daily) regression coefficients from matchups falling within specified time windows. Typical sizes of time windows are 1±45 days for GR SST and 1±180 days for PWR SST, with the offsets of regression equations being additionally corrected using shorter time windows containing at least 100 matchups. The larger window size for PWR SST is intended to provide sufficient numbers of matchups for specific segments in the **R**-space. At the next run, the full mission is reprocessed with variable coefficients and adjusted ACSM filters. The iterations with continuous recalculation of the coefficients are repeated until changes in retrieved SST between sequential runs become small.

The method for deriving regression coefficients from matchups [8] accounts for two important features of Eqs. (1-2). First, according to the conventional NLSST approach [9], the equations include regressors depending on T_0. Since the correlation between T_0 and T_{IS} is usually very high (>0.9), the inclusion of such regressors in the equation improves precision of fitting T_{IS} with T_S. The improvement in precision is even more noticeable in PWR SST, because correlations of T_0-independent regressors with T_{IS} are in general lower over segmental subsets of matchups than within a global MDS. The drawback of using T_0-dependent regressors is that T_S becomes sensitive to T_0, while its sensitivity to T_{SKIN} may degrade. The method [8] preserves the sensitivity of GR SST to T_{SKIN} and, at the same time, reduces the sensitivity to T_0 by posing a constraint on mean sensitivity over the training MDS, $<\mu>$. In RAN2 B01, we used for GR SST the constraint $<\mu> = 0.94$ for day and $<\mu>=0.98$ for night. For the PWR SST, the segmental coefficients were initially calculated without constraint on $<\mu>$. If the segmental value of $<\mu>$ with unconstrained coefficients was less than 0.4 then the coefficients were recalculated under the constraint $<\mu>=0.4$. Second, one can notice that Eqs. (1-2) include more terms than the equations adopted at the Ocean and Sea Ice Satellite Application Facility (OSI-SAF) [18,19] and later implemented in ACSPO for S-NPP VIIRS [6], as well as for MODIS and AVHRR. The increased numbers of regressors help extract the maximum information from satellite observations. The risk of adding more regressors in the equation, however, is that due to increased correlations between regressors within the training MDS, the estimated coefficients, produced with the conventional least-squares method, may become unstable. The method [8] reduces the dimensionality of the subspace, in which the vector of coefficients is sought for, by cutting off the least informative dimensions in the **R**-space. This ensures extracting the maximum information from the regressors while keeping the estimates of coefficients stable.

4. ACSPO CLEAR-SKY MASK (ACSM)

The ACSPO Clear-Sky Mask (ACSM) is the key element of the SST system, responsible for cloud screening and quality control of SST retrievals [5]. In RAN2 B01, the ACSM employs eight threshold-based filters. The following five filters use retrieved SSTs or BTs in the AVHRR IR bands as predictors:

1. SST filter (includes static and adaptive parts)
2. Warm SST filter for low stratus clouds
3. Low stratus filter
4. Uniformity filter
5. Warm Outliers filter

The above five filters are used during both day and night. The fifth "Warm Outliers" filter was developed specifically for RAN2 B01. It is discussed in Section 5. The ACSM also includes three daytime filters:

    6.   Reflectance Relative Contrast filter
    7.   Reflectance "Gross" Contrast filter
    8.   SST/Reflectance Cross-Correlation filter

The filters 6 and 7 use AVHRR reflectance bands 1 (0.63 µm) and 2 (0.87 µm). The filter 8 exploits cross correlation between reflectance in band 1 and GR SST. All filters are binary, with output being either "clear" or "cloudy". The definitions of quality levels (QL) in ACSPO are based on the ACSM individual bit flags. Only QL=5 is recommended for use in all applications, which is assigned to pixels for which all filters show "clear". Except including the new "Warm Outliers" filter, the main modification of the ACSM during RAN2 B01 has been making the SST filter more conservative for NOAA-11 and NOAA-12 in mid-1991 to 1992, to mitigate the effect of contamination of the atmosphere with the volcanic dust following two eruptions of Mt. Pinatubo and Mt. Hudson in 1991. This was a temporary solution, which will be revisited in the future betas of RAN2.
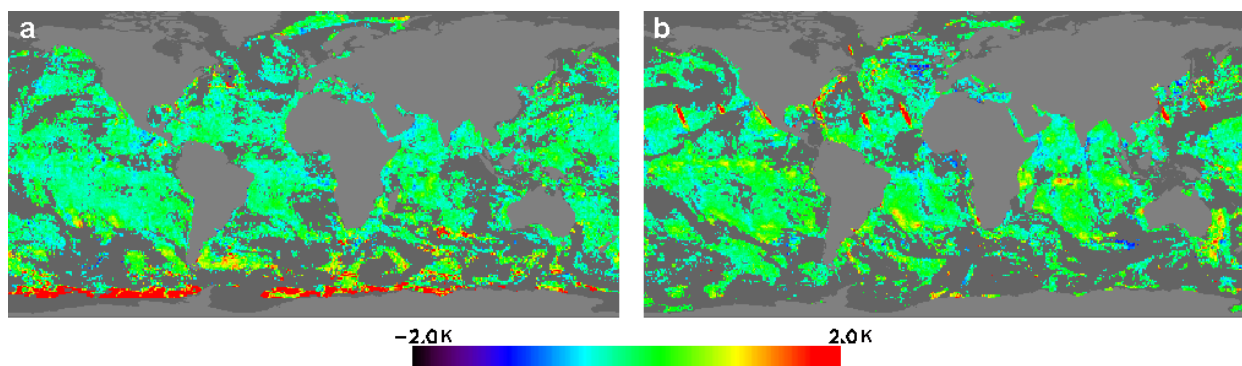
5.   THE WARM OUTLIERS FILTER

Figure 2. Deviations of nighttime GR SSTs from CMC for (a) NOAA-14 AVHRR/2 data on 20 Jan 1996 and (b) NOAA-15 AVHRR/3 on 15 Feb 1999 with NRT ACSPO, before applying the "Warm Outliers" filter.

Initial processing of RAN2 B01 AVHRR data with the NRT ACSPO revealed significant warm outliers in nighttime SSTs, retrieved with the three-band Eq. (2). These outliers are caused by obviously erroneous BTs reported in the band 3b due to occasional Sun stray light and impingement on the black body in those "twilight" pixels, for which SZA > 90°, i.e. the Earth's surface is not illuminated by the Sun, but the satellite is, when in a near-terminator orbit [18]. As shown in Fig. 2, locations of such outliers vary for different satellites. In Fig. 2a, large warm deviations of NOAA-14 GR SST from CMC appear in Southern high latitudes. In Fig. 2b, the warm outliers in NOAA-15 GR SST are seen in the northern hemisphere at the western edges of the AVHRR swaths. It is difficult to predict exactly in which nighttime pixels the conditions for such outliers will be met, because this would require accurate knowledge of satellite position and orientation of the sensor with respect to the Sun. In RAN1 B01, we have empirically developed a number of sensor-specific "Warm Outliers" filters, to identify and screen out the outliers of this type. For each satellite, we define ranges of SZA, VZA and latitudes, within which the warm outliers may occur. Then the set of suspicious pixels is thinned out using three following predictors:

1. A differential part of Eq. (2), i.e., a set of terms depending on the brightness temperature differences:

$$\Delta T = b_2(T_{11}-T_{3.7}) + b_3(T_{11}-T_{12}) + b_5(T_{11}-T_{3.7})S + b_6(T_{11}-T_{12})S + b_7(T_{11}-T_{3.7})T_0 + b_8(T_{11}-T_{12})T_0.$$

Too large values of ΔT usually indicate erroneous BTs, which cause SST outliers.

2. Fisher distance ρ - a measure of consistency of a given vector of regressors with the global training MDS [7]. Too large values of ρ typically correspond to unlikely vectors of regressors. The Fisher distance is calculated in ACSPO for each ocean pixel as a function of **R**.

3. The difference between retrieved SST and T_0, T_S - T_0.

The pixels, for which $\Delta T > D$, $\rho > P$ and T_S - $T_0 > \delta$, are classified as outliers. The thresholds D, P and δ, as well as suspicious ranges of SZA, VZA and latitudes, are determined empirically for each satellite.

6. EXAMPLES OF RAN2 B01 SST RETRIEVALS

We illustrate the performance of the RAN2 B01 SST with examples of SST retrievals from NOAA-14 and NOAA-15. Detailed evaluation of the RAN2 B01 SST is found in [4].

Figs. 3-4 show maps of GR-CMC and PWR-CMC SSTs from NOAA-14 for 20 Jan 1996 and NOAA-15 for 15 Feb 1999. Tables 2-3 summarize their global statistics, along with corresponding clear-sky fractions (ratio of a number of clear-sky pixels to a total number of ice-free ocean pixels). Comparisons of nighttime GR SSTs in Figs. 3-4c with Fig. 2 show that in both cases the "Outliers" filter effectively screens out the warm SST outliers. Filtering outliers reduces the clear-sky fractions by ~1%, while significantly reducing the corresponding standard deviations (SD) of both GR-CMC and PWR-CMC SSTs. The manifestations of diurnal warming events and cloud leakages, more noticeable in GR SST, are suppressed in PWR SST. As a result, the SDs of PWR-CMC are much smaller than SDs of GR-CMC SST.

Figs. 5-6 show geographical distributions of the corresponding GR SST sensitivities, and Table 4 shows their global statistics. Note that daily global mean sensitivity, averaged over all clear-sky ocean pixels, may deviate from the mean sensitivity over the training MDS (which recall were constrained to 0.94 for day and 0.98 for night). During the day, the GR sensitivity degrades in the tropics and reaches 0.7 at large VZAs (cf. [6]). The nighttime sensitivity is less variable.

Figs. 7-8 show the time series of daily biases and SDs of GR and PWR SSTs with respect to *in situ* SST, for the whole NOAA-14 mission. Note that Fig. 7 was produced using fixed regression coefficients, derived from matchups collected during the whole year of 1996, whereas Fig. 8 with variable (daily) regression coefficients, trained on matchups collected within the sliding time windows as described in Section 3. Switching from fixed to variable coefficients significantly reduces variations in SST biases, as expected, whereas the SDs remain largely unchanged. During the day, the average daily SDs with respect to *in situ* SST are close to ~0.45 K for GR and ~0.35 K for PWR SST. At night, these SDs are ~0.40 K for GR and ~0.30 K for PWR SST, respectively.

Fig. 9 shows time series of nighttime bias and SD of NOAA-14 GR and PWR SSTs with respect to *in situ* SST, produced with the same variable coefficients as in Fig.8 (a, b), but without applying the "Warm Outliers" filter. Comparison with Fig. 8 (c, d) shows the importance of filtering SST outliers. If not filtered, they significantly deteriorate the statistics of both GR and PWR SSTs.

Table 2. Biases and SDs of GR/PWR – CMC SST and clear-sky fractions from NOAA-14 on 20 Jan 1996 (fixed coefficients).

Statistics	Day	Night (RAN2 B01)	Night (No warm outlier filter)
Bias, GR – CMC SST	+0.20 K	+0.03 K	+0.18 K
SD, GR – CMC SST	0.64 K	0.46 K	0.78 K
Bias, PWR – CMC SST	+0.17 K	+0.00 K	+0.00 K
SD, PWR – CMC SST	0.42 K	0.31 K	0.79 K
Clear-sky fraction	14.5%	14.3%	15.6%

Table 3. Same as in Table 2 but for NOAA-15 on 15 Feb 1999.

Statistics	Day	Night (RAN2 B01)	Night (No warm outlier filter)
Bias, GR – CMC SST	-0.07 K	+0.14 K	+0.17 K
SD, GR – CMC SST	0.49 K	0.48 K	0.58 K
Bias, PWR – CMC SST	-0.09 K	+0.12 K	+0.15 K
SD, PWR – CMC SST	0.34 K	0.30 K	0.37 K
Clear-sky fraction	13.7%	16.9%	18.1%

GR SST - CMC, DAY

PWR SST - CMC, DAY
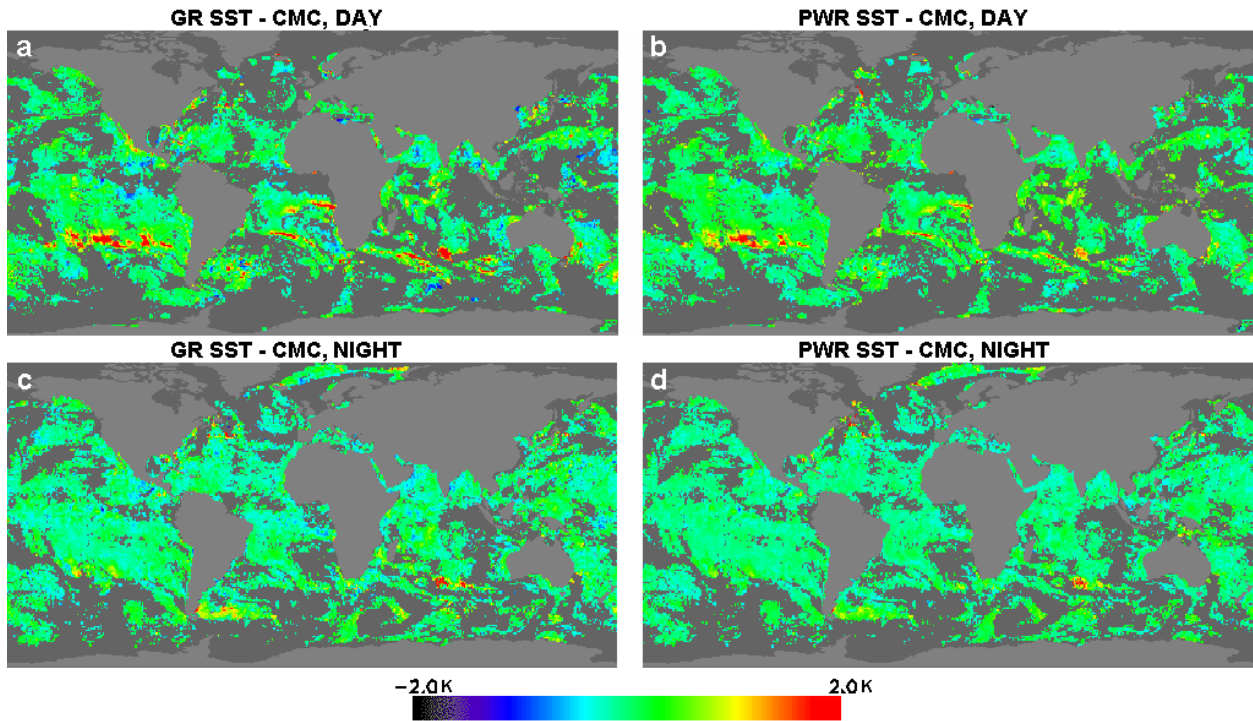
GR SST - CMC, NIGHT

PWR SST - CMC, NIGHT

−2.0 K   2.0 K

Figure 3. (a,b) Daytime and (c,d) nighttime (a,c) GR-CMC and (b,d) PWR-CMC SSTs for NOAA-14 on 20 Jan 1996 in RAN2 B01.

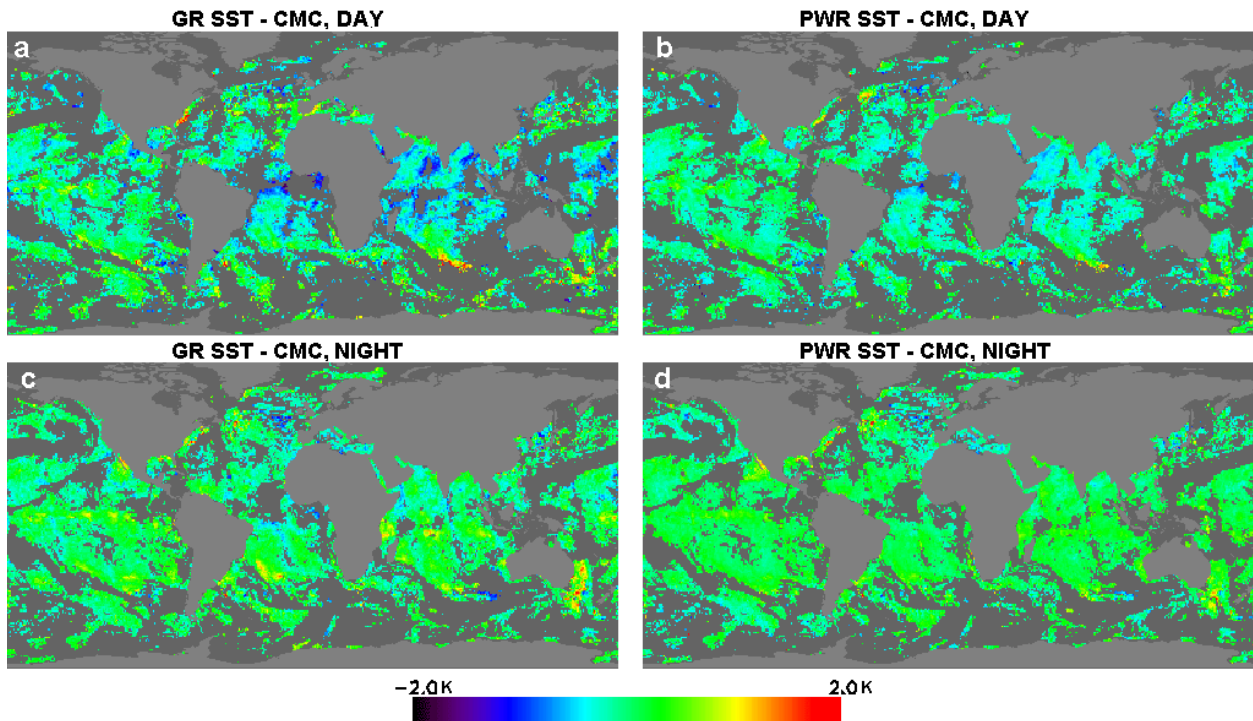**GR SST - CMC, DAY**

PWR SST - CMC, DAY

GR SST - CMC, NIGHT

PWR SST - CMC, NIGHT

−2.0 K   2.0 K

Figure 4. Same as in Fig. 3 but for NOAA-15 on 15 Feb 1999.

7. SUMMARY AND FUTURE WORK

The initial "B01" version of RAN2 AVHRR SST dataset, covering 1981-2002 was created from data of NOAA-07, 09, 11, 12, 14, 15 and 16. It includes two SST products: the Global Regression (GR) SST, sensitive to T_{SKIN}, but de-biased with respect to "depth" SST, and denominated as "sub-skin" SST; and the Piecewise Regression (PWR) SST, which is more accurate and precise with respect to *in situ SST*. This product serves in ACSPO as proxy for T_{DEPTH}.

In RAN2 B01, we have addressed specific issues intrinsic to the AVHRR observations during 1981-2002:

- Instabilities in AVHRR data were mitigated by recalculation of regression coefficients on a daily basis from matchups collected within sliding time windows centered at a given day. The training method provided stable estimates of regression coefficients and maintained the mean sensitivity of GR SST to "skin" SST at ~0.94 for two-band SST retrieval and ~0.98 for three-band retrieval.
- The effects of Sun stray light and impingement on the black body in band 3/3b has been mitigated by identifying and screening out nighttime warm outliers in GR SST.
- The critical shortage of *in situ* data from drifters and moored buoys needed for training SST algorithms for NOAA-07, 09 and 11, was compensated with more numerous SST measurements from ships.

The future development of RAN2 SST algorithms will be aimed at mitigation of cold regional biases in retrieved SST caused by contamination of the atmosphere with volcanic dust after eruptions of El Chichon in Mar-Apr 1982 (which affected NOAA-07 observations) and Mt. Pinatubo in June 1991 and Mt. Hudson in Aug-Oct 1991 (which affected observations from NOAA-11 and -12). The cold biases may be also caused by sensor anomalies. In many cases, the cold biases have well-expressed latitudinal dependencies. We will try to mitigate cold biases, at least, in two ways: by accounting for latitudinal dependencies in the Clear-Sky mask and by correction of AVHRR BTs using calibration parameters, available in L1b data.
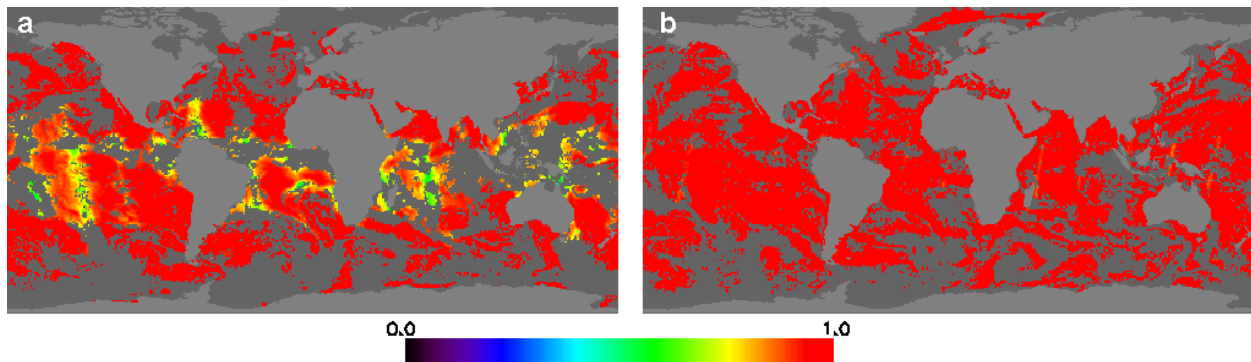

Figure 5. (a) Daytime and (b) nighttime sensitivities of NOAA-14 GR SST on 20 Jan 1996.
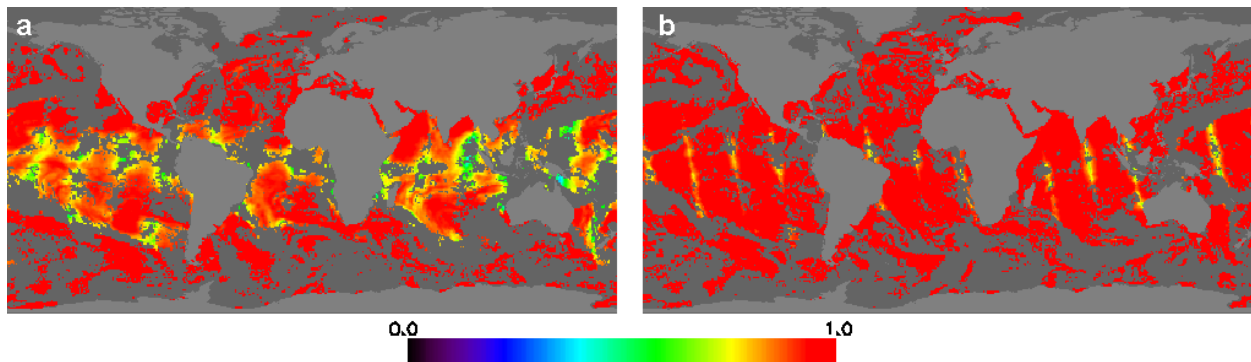

Figure 6. (a) Daytime and (b) nighttime sensitivities of NOAA-15 GR SST on 15 Feb 1999.
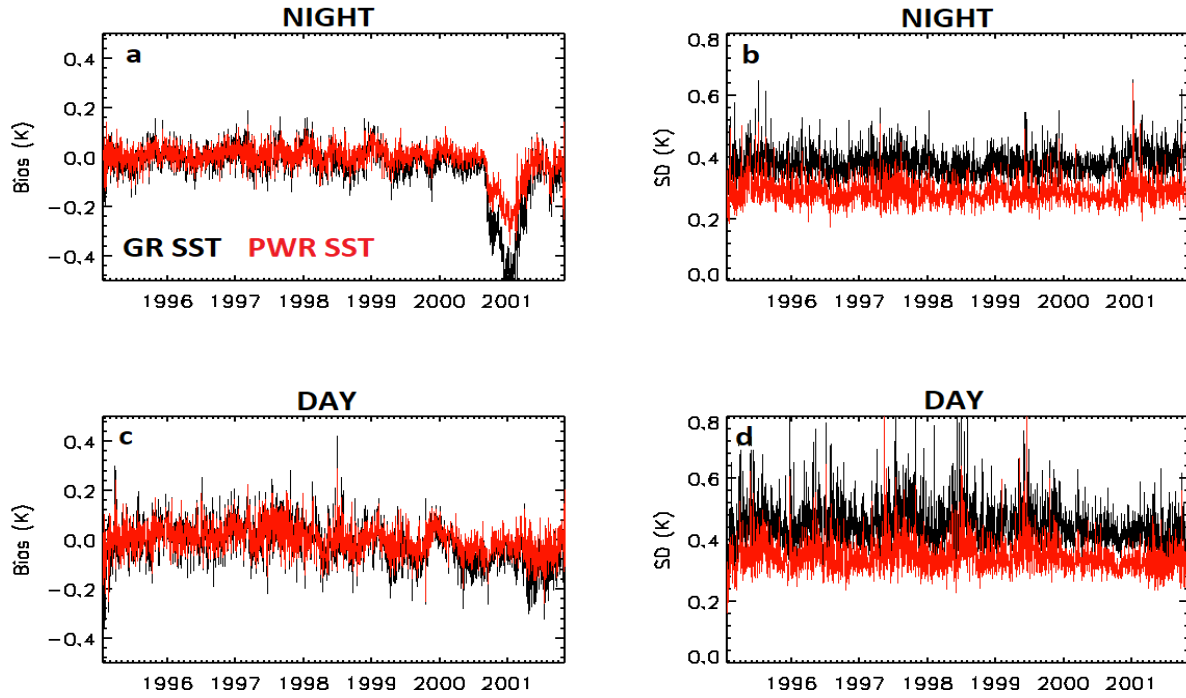
Figure 7. Time series of (a, b) nighttime and (c, d) daytime daily global (a, c) biases and (b, d) standard deviations of GR and PWR SSTs with respect to in situ SST, produced from NOAA-14 AVHRR with fixed regression coefficients.
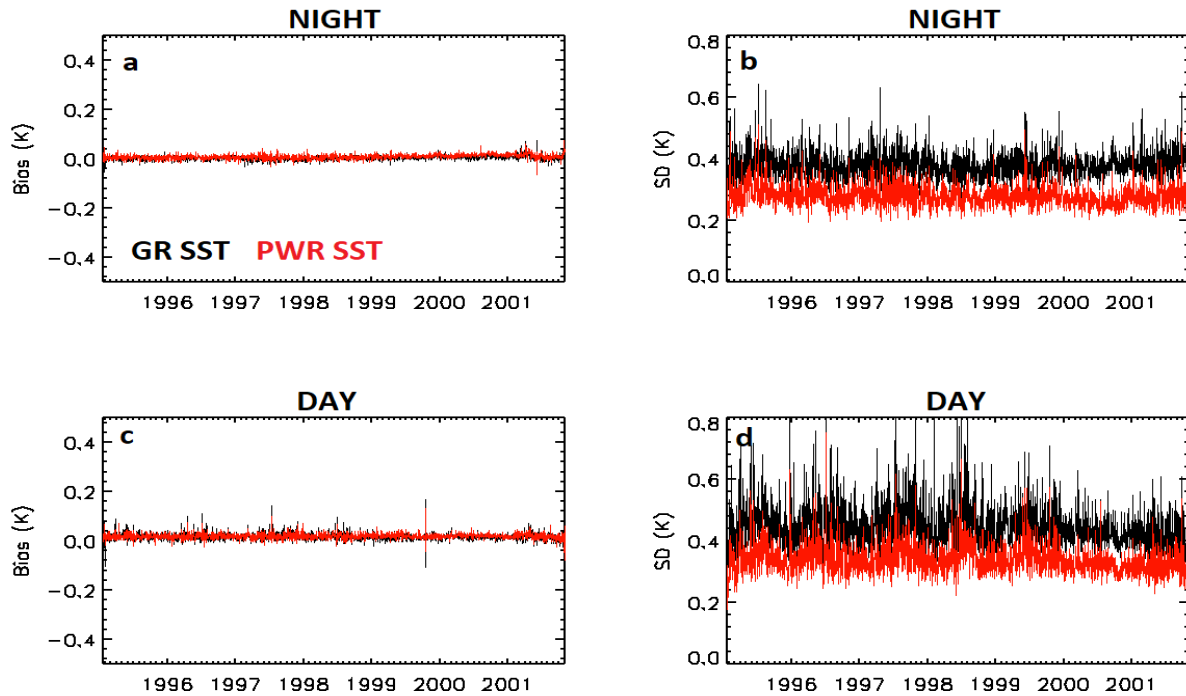

Figure 8. Time series of (a, b) nighttime and (c, d) daytime daily global (a, c) biases and (b, d) standard deviations of GR and PWR SSTs with respect to in situ SST, produced from NOAA-14 AVHRR with variable regression coefficients.

Proc. of SPIE Vol. 11420 1142004-9

Table 4. Global means and SDs of GR SST sensitivities for NOAA-14 on 20 Jan 1996 and NOAA-15 on 15 Feb 1999.

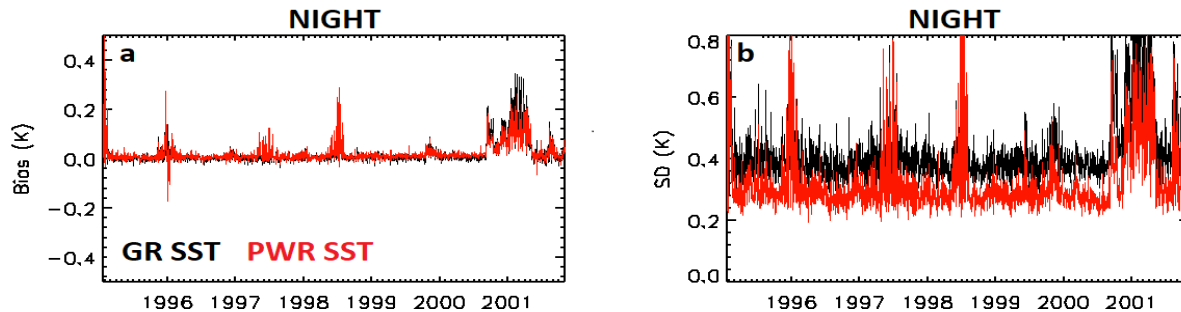| GR SST sensitivity	Day	Night
NOAA-14, 20 Jan 1996		
Mean	0.95	0.99
SD	0.06	0.02
NOAA-15, 15 Feb 1999		
Mean	0.91	0.97
SD	0.07	0.03

Figure 9. Same as in Fig. 8 (a, b), but produced before filtering warm SST outliers caused by artifacts in band 3b.

ACKNOWLEDGEMENTS

REFERENCES

[1]   Ignatov, A., Zhou, X., Petrenko, B., Liang, X., Kihai, Y., Dash, P., Stroup, J., Sapper, J. and DiGiacomo, P., "AVHRR GAC SST Reanalysis Version 1 (RAN1)," *Remote Sens.*, **8**, 315, doi: 10.3390/rs8040315 (2016).

[2]   Kilpatrick, K., Podesta, G., and Evans, R., "Overview of the NOAA/NASA advanced very high resolution radiometer Pathfinder algorithm for sea surface temperature and associated matchup database," *JGR*, **106**, *C5*, 9179-9199, doi: 10.1029/1999JC000065 (2001).

[3]   Merchant, C., Embury, O., Bulgin, C., et al., "Satellite-based time-series of sea-surface temperatures since 1981 for climate applications", *Scientific Data*, 6:223, doi: 10.1038/s41597-019-0236-x (2019).

[4]   Pryamitsyn, V., Ignatov, A., Petrenko, B., Jonasson, O., Pennybacker, M. and Kihai, Y., "Evaluation of the initial NOAA AVHRR GAC Reanalysis Version 2 (RAN2)". Proc. SPIE, Anaheim, 26-30 April 2020 (2020).

[5]   Petrenko, B., Ignatov, A., Kihai, Y., and Heidinger, A., "Clear-sky mask for the Advanced Clear-Sky Processor for Oceans", *JTECH*, **27**, 1609–1623, doi: 10/1175/2010JTECHA1413.1 (2010).

[6]   Petrenko, B., Ignatov, A., Kihai, Y., et al., "Evaluation and selection of SST regression algorithms for JPSS VIIRS", *JGR*, **119**, 4580-4599, doi: 10.1117/12.2017454 (2016).

[7]   Petrenko, B., Ignatov, A., Kihai, Y., and Dash, P., "Sensor-Specific Error Statistics for SST in the Advanced Clear-Sky Processor for Oceans", *JTECH*, **33**, 345-359, doi: 10.1175/JTECH-D-15-0166.1 (2016).

[8]   Petrenko, B., Ignatov, A., Kramar, M. and Kihai, Y., "Exploring new bands in modified multichannel regression SST algorithms for the next-generation infrared sensors at NOAA," *Proc. SPIE*, **9827**, 98270N-1, doi: 10.1117/12.2229578 (2016).

[9] He, K., Ignatov, A., Kihai, Y., Cao, C., and Stroup, J., "Sensor Stability for SST (3S): Toward Improved Long-Term Characterization of AVHRR Thermal Bands", *Remote Sens.*, **8**, 346, doi: 10.3390/rs8040346 (2016).

[10] Xu, F., Ignatov, A., "*In situ* SST Quality Monitor (*i*Quam)". *JTECH,* doi: 10.1175/JTECH-D-13-00121.1 (2014).

[11] Dash, P., Ignatov, A., Kihai, Y., Sapper, J., "The SST Quality Monitor (SQUAM)," *JTECH*, **27**, 1899-1917, doi: 10.1175/2010JTECHO756.1 (2010).

[12] Xu, F., Ignatov, A., "Error characterization in *i*Quam SSTs using triple collocations with satellite measurements", *GRL,* https://doi.org/10.1002/2016GL070287 (2016).

[13] Walton, C.C., Pichel, W.G., Sapper, J.F., and May, D.A., "The development and operational application of nonlinear algorithms for the sea surface temperatures with the NOAA polar-orbiting environmental satellites", *JGR*, **103**, 27999–28012, doi: 10.1029/98JC02370 (1998).

[14] Brasnett, B., Surcel Colan, D., "Assimilating retrievals of sea surface temperature from VIIRS and AMSR2", *JTECH*, **33**, 361-375, doi: 10.1175/JTECH-D-15-0093.1 (2016).

[15] Liang, X., Ignatov, A., Kihai, Y., "Implementation of the Community Radiative Transfer Model (CRTM) in Advanced Clear-Sky Processor for Oceans (ACSPO) and validation against nighttime AVHRR radiances", *JGR*, **114**, D06112, doi: 10.1029/2008JD010960 (2009).

[16] Gelaro, R., et al., "The modern-era retrospective analysis for research and applications, version 2 (MERRA-2)", *J. Clim.*, **30**, 5419–5454, doi: 10.1175/JCLID-16-0758.1 (2017).

[17] Liang, X., Ignatov, A., "Monitoring of IR Clear-Sky Radiances over Oceans for SST (MICROS)," *JTECH*, **28**, 1228-1242, doi: 10.1175/JTECH-D-10-05023.1 (2011).

[18] Brisson, A., Le Borgne, P. and Marsouin, A., "Results of one year of preoperational production of SST from GOES-8", *JTECH*, **19**, 1638–1652, doi: 10.1175/1520-0426(2002)019<1638:ROOYOP>2.0.CO;2 (2002).

[19] "OSI-SAF Low Earth Orbiter Sea Surface Temperature Product User Manual, Version 2.1", EUMETSAT OSI-SAF, http://www.osi-saf.org/biblio/docs/ss1_pum_leo_sst_2_1.pdf (2009).